

## Effects of density-dependent weak form factors on charged-current neutrino-nucleus scattering in the quasi-elastic region

K. S. Kim

*School of Liberal Arts and Science, Korea Aerospace University, Goyang 412-791, Korea*

Myung-Ki Cheoun

*Department of Physics, Soongsil University, Seoul 156-743, Korea*

W. Y. So

*Department of Radiological Science, Kangwon National University, Samcheok 245-711, Korea*

(Received 10 June 2013; revised manuscript received 18 June 2014; published 10 July 2014)

We study the effects of density-dependent electromagnetic, axial, and weak vector form factors on the inclusive ( $e, e'$ ) reaction and the charged-current neutrino-nucleus scattering in the quasi-elastic region within the framework of a relativistic single-particle model. The density-dependent form factors obtained from a quark-meson coupling model are applied into the ( $e, e'$ ) reaction and the neutrino-nucleus scattering via charged current. The effects of the density-dependent form factors increase the ( $e, e'$ ) cross sections by a few percent. However, the effects may reduce the differential cross sections up to 20% (60%) at  $\rho = 1.0\rho_0$  ( $2.0\rho_0$ ) for the antineutrino scattering and also reduce the cross section up to 20% (30%) at  $\rho = 1.0\rho_0$  ( $2.0\rho_0$ ) for the neutrino scattering around the peak positions, where the normal density is  $\rho_0 \sim 0.15 \text{ fm}^{-3}$ . For the density of finite nuclei such as  $^{12}\text{C}$ ,  $^{40}\text{Ca}$ , and  $^{208}\text{Pb}$  as 0.6, 0.7, and 1.0 of  $\rho_0$ , the in-medium effects are 20% to 30%, even in the antineutrino case. Our theoretical double-differential and total cross sections are compared with the recent MiniBooNE data for  $^{12}\text{C}(\nu_\mu, \mu^-)$  scattering.

DOI: [10.1103/PhysRevC.90.017601](https://doi.org/10.1103/PhysRevC.90.017601)

PACS number(s): 25.30.Pt, 13.15.+g, 24.10.Jv

Since the “EMC” effect [1] was first discovered, the possible medium modifications of nucleon form factors have been studied for over thirty years. During the last twenty years, two different theoretical models have appeared to predict the modifications of the electric and magnetic form factors of nucleons in a nuclear medium. These are the quark-meson coupling (QMC) model generated by Thomas and collaborators [2], and the cloudy bag model (CBM) used by Cheon and Jeong [3]. In nuclear media, both models tend to show a more rapid falloff with four-momentum transfer squared ( $Q^2$ ) for the electric form factor  $G_E$  than the free-space value.

An experiment at the Thomas Jefferson National Accelerator Facility JLab [4] obtained the ratio of  $G_E/G_M$  for protons by measuring  $P_t$  and  $P_l$ , which are the transverse and the longitudinal recoil proton polarization, respectively, in  $\bar{e}p \rightarrow e\bar{p}$  scattering at high  $Q^2$  (0.5–3.5 GeV/ $c^2$ ). Subsequent experiments  $^4\text{He}(\bar{e}, e'\bar{p})^3\text{H}$  at the Mainz Microtron (MAMI) at  $Q^2 = 0.4 \text{ GeV}/c^2$  [5] and JLab [6,7] at 0.5–3.5 GeV/ $c^2$  investigated the polarization transfer reaction and extracted the ratio of the polarization transfer ratio ( $P'_x/P'_z$ ) for  $^4\text{He}$  over the same ratio for  $^1\text{H}$ . Since the polarization transfer ratio is proportional to  $G_E/G_M$ , medium effects might change the value of the ratio for a proton in  $^4\text{He}$  as compared to a free proton.

As for theoretical calculations, Kim and Cheoun [8] investigated the roles of the anomalous magnetic moment in a nuclear medium within the CBM model and found no explanation of a possible longitudinal suppression for inclusive ( $e, e'$ ) reaction from  $^{40}\text{Ca}$  and  $^{208}\text{Pb}$  at lower electron energy. To investigate the medium effects of the nucleon electric

and magnetic (EM) form factors in the nucleus, Kim and Wright [9] calculated the quasi-elastic electron scattering and found no discernible evidence for the modification of the nucleon form factors from their free-space values for the inclusive ( $e, e'$ ) reactions. Cloet *et al.* [10] addressed, in the  $^4\text{He}(\bar{e}, e'\bar{n})^3\text{He}$  reaction, that the in-medium change of the  $G_E/G_M$  form-factor ratio for a bound neutron at small values of momentum transfer,  $Q^2$ , is dominated by the change in the electric-charge radius

On the other hand, the Adelaide group [11] calculated the weak form factors with density-dependence in the QMC model. This model successfully described various properties of hadrons in a nuclear medium, finite nuclei [12], and hypernuclei [13]. In particular, the authors of Ref. [12] found a simple scaling relationship for the change of the hadron masses, which was described in terms of the number of nonstrange quarks in a hadron and the value of the scalar mean field in a nucleus.

In our previous papers [14], we study the effects of density-dependent form factors on the neutrino reaction via charged current (CC) and neutral current (NC) within the framework of the quasiparticle random phase approximation (QRPA). Neutrino-reaction cross sections in a nuclear medium with normal density  $\rho_0$  can be reduced by about 5% maximally, but antineutrino-reaction cross sections are largely decreased in the nuclear medium by around 30% because of different helicities. But these calculations were performed for neutrino reactions at  $E_{\nu(\bar{\nu})} \leq 80 \text{ MeV}$ .

Recently, since the first measurement of  $^{12}\text{C}(\nu_\mu, \mu^-)$  scattering at MiniBooNE [15], several theoretical works have appeared [16–18]. Nieves *et al.* [16] calculated the double

cross section by including multinucleon contributions and then deduced the increase of the axial mass associated with the concept of underestimated neutrino flux. To explain the MiniBooNE data, Meucci *et al.* [17] obtained a good description of the total cross section by using the relativistic Green's function method. Ankowski [18] calculated  $^{12}\text{C}(\nu_\mu, \mu^-)$  scattering with the axial mass 1.23 GeV and underestimated the MiniBooNE data by 20%, but overestimated the data by 15% with an axial mass of 1.39 GeV.

In the present work, we investigate the in-medium effects by the density-dependent weak form factors by examining the inclusive  $(e, e')$  reaction and the inclusive CC neutrino(antineutrino)-nucleus  $[\nu(\bar{\nu})-A]$  scattering from  $^{12}\text{C}$ ,  $^{40}\text{Ca}$ , and  $^{208}\text{Pb}$ . We use a relativistic single-particle model in the quasi-elastic region. The bound nucleon wave functions are solutions to the Dirac equation in the presence of the strong scalar and vector potentials of the  $\sigma$ - $\omega$  model [19]. The wave functions of the nucleons knocked out are generated by the same potential as for the bound nucleons, which is called the relativistic mean field (RMF). This RMF model has been widely used to calculate the electron- and neutrino-nucleus scattering [20]. This RMF model guarantees current conservation and gauge invariance and provides good agreement with the Bates  $(e, e')$  data by approximating the Coulomb distortion for incoming and outgoing electrons [21]. In particular, in order to include the Coulomb distortion of the outgoing leptons, we use the approach of our previous work [22]. Our results are compared with double-differential and total-cross-section data measured by MiniBooNE [15].

We choose a laboratory frame where the target nucleus is seated at the origin of the coordinate system. Four-momenta of incident and outgoing  $\nu(\bar{\nu})$  are labeled  $p_i^\mu = (E_i, \mathbf{p}_i)$ ,  $p_f^\mu = (E_f, \mathbf{p}_f)$ .  $p_A^\mu$ ,  $p_{A-1}^\mu$ , and  $p^\mu$  represent the four-momenta of the target nucleus, residual nucleus, and final nucleon, respectively. The differential cross section is given by

$$\frac{d\sigma}{dT_N} = 4\pi^2 \frac{M_N M_{A-1}}{(2\pi)^3 M_A} \int \sin\theta_l d\theta_l \int \sin\theta_N d\theta_N p f_{\text{rec}}^{-1} \sigma_M^W \times [v_L R_L + v_T R_T + h v'_T R'_T], \quad (1)$$

where  $M_N$  is the nucleon mass,  $\theta_l$  denotes the scattering angle of the lepton, and  $h = -1$  ( $h = +1$ ) corresponds to the helicity of the incident  $\nu$  ( $\bar{\nu}$ ).  $\theta_N$  and  $T_N$  represent the polar angle and the kinetic energy of the knocked-out nucleons, respectively. Detailed forms for the kinematical factor  $\sigma_M^W$ , recoil factor  $f_{\text{rec}}$ , kinematical coefficients  $v$ , and the corresponding response functions  $R$  are given in our previous paper [23].

For a free nucleon, the weak current operator  $\hat{J}^\mu$  for the CC reaction comprises the vector  $F_i^V(Q^2)$ , the axial  $G_A(Q^2)$  vector, and the pseudoscalar  $G_P(Q^2)$  form factors given by

$$\hat{J}^\mu = F_1^V(Q^2)\gamma^\mu + F_2^V(Q^2)\frac{i}{2M_N}\sigma^{\mu\nu}q_\nu + G_A^{CC}(Q^2)\gamma^\mu\gamma^5 + \frac{G_P(Q^2)}{2M}q^\mu\gamma^5. \quad (2)$$

By the conservation of vector current hypothesis, the vector form factors for the CC reaction are expressed as

$$F_i^{V,p(n)(CC)} = F_i^{p(n)}(Q^2) - F_i^{n(p)}(Q^2). \quad (3)$$

The axial form factor is usually given by

$$G_A^{CC}(Q^2) = -g_A/(1 + Q^2/M_A^2)^2, \quad (4)$$

where  $g_A = 1.262$  and  $M_A = 1.032$  GeV represent the axial coupling constant and the axial cutoff mass, respectively. The induced pseudoscalar form factor is parametrized by the Goldberger–Treiman relation:

$$G_P(Q^2) = \frac{2M_N}{Q^2 + m_\pi^2} G_A^{CC}(Q^2), \quad (5)$$

where  $m_\pi$  is the pion mass.

In this work, we put the density-dependence of the weak form factors,  $R(F_{1,2}^V) = F_{1,2}^V(\rho, Q^2)/F_{1,2}^V(\rho = 0, Q^2)$ , which is generated by the QMC model [11]. The constituent quark mass in a hadron is generated by the quark condensate  $\langle \bar{q}q \rangle$  in vacuum, but the mass (or  $\langle \bar{q}q \rangle$ ) in nuclear matter may be reduced from the value in vacuum because of the condensed scalar ( $\sigma$ ) field depending on the nuclear density  $\rho$ . The decrease of the quark mass then leads to the variation of baryon internal structures at the quark level. Such an effect is considered self-consistently in the QMC model. Detailed features of the form factors and their modifications in nuclear matter used in this study are found in Ref. [14].

As shown in Fig. 1, we calculate the inclusive  $(e, e')$  reaction in terms of the energy transfer  $\omega$  before we calculate the  $\nu(\bar{\nu})$ - $A$  scattering by comparing with the experimental data from the Stanford Linear Accelerator Center (SLAC) [24]. Solid (red) curves are the results for no density dependence, dashed (black) curves are for  $\rho = 0.5\rho_0$ , dotted (blue) curves are for  $\rho = \rho_0$ , dash-dotted (pink) curves are for  $\rho = 1.5\rho_0$ , dash-dot-dotted (sky blue) curves are for  $\rho = 2.0\rho_0$ .

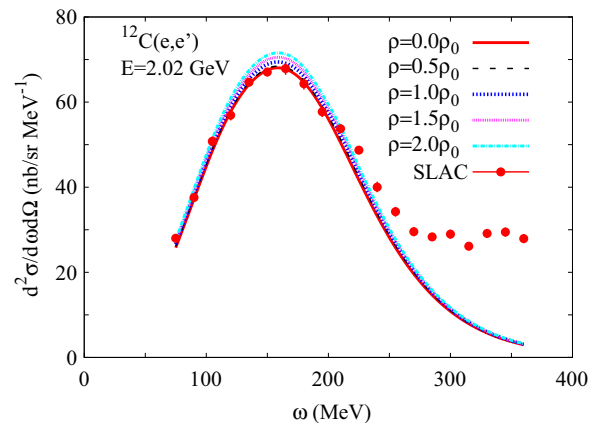


FIG. 1. (Color online) The differential cross sections of the inclusive  $(e, e')$  reaction in terms of the energy transfer  $\omega$  for the incident electron energy 2.02 GeV and scattering angle  $\theta = 15^\circ$  from  $^{12}\text{C}$ . Solid (red) curves are the results for no density dependence, dashed (black) curves are for  $\rho = 0.5\rho_0$ , dotted (blue) curves are for  $\rho = \rho_0$ , dash-dotted (pink) curves are for  $\rho = 1.5\rho_0$ , dash-dot-dotted (sky blue) curves are for  $\rho = 2.0\rho_0$ . The experimental data were measured at the Stanford Linear Accelerator Center [24].

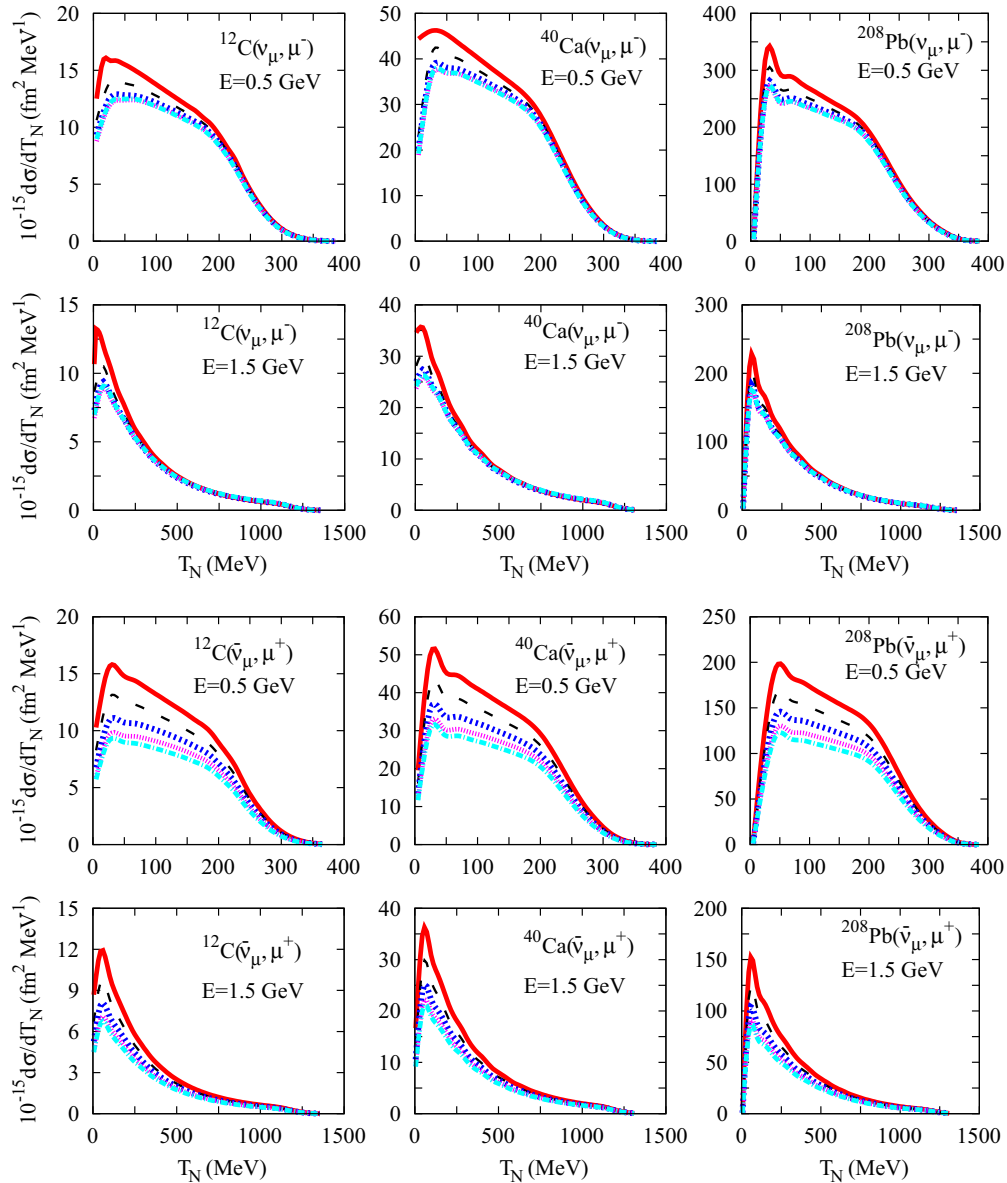


FIG. 2. (Color online) The differential cross sections of the neutrino scattering for the incident neutrino energies 0.5 and 1.5 GeV from  $^{12}\text{C}$ ,  $^{40}\text{Ca}$ , and  $^{208}\text{Pb}$ . The explanations of the curves are the same as for Fig. 1. The upper six panels are the results for the neutrino and the lower six are for the antineutrino.

and dash-dot-dotted (sky-blue) curves are for  $\rho = 2.0\rho_0$ . The differences between each curve are 1%  $\sim$  2% and the effect of the density enhances the cross section with higher densities. This result shows reverse behavior of the nuclear medium effect by changing the nucleon form factor in our previous work [9]. Note that the  $\rho_0 \sim 0.15 \text{ fm}^{-3}$  is the normal density. But, if we take  $^{12}\text{C}$  density as  $\rho = 0.6\rho_0$ , this density dependence is not discernible in the electron scattering.

In Fig. 2, we calculate the differential cross sections for the  $\nu(\bar{\nu})$ - $A$  scattering in terms of the kinetic energy of the knocked-out nucleons from  $^{12}\text{C}$ ,  $^{40}\text{Ca}$ , and  $^{208}\text{Pb}$  at incident-neutrino energies of 0.5 and 1.5 GeV. Solid (red) curves are the results for no density dependence, dashed (black) curves are for  $\rho = 0.5\rho_0$ , dotted (blue) curves are for  $\rho = 1.0\rho_0$ , dash-dotted (pink) curves are for  $\rho = 1.5\rho_0$ ,

dash-dot-dotted (sky-blue) curves are for  $\rho = 2.0\rho_0$ . The upper six panels are the results for  $\nu$  and the lower six are for  $\bar{\nu}$ .

For the case of  $\nu$ , around the peak positions, the effects of the density-dependent form factors reduce the cross sections by about 10% for  $\rho = 0.5\rho_0$ , 20% for  $\rho = 1.0\rho_0$ , 30% for  $\rho = 1.5\rho_0$ , and 30% for  $\rho = 2.0\rho_0$ . The effects do not depend on the incident  $\nu$  energies and nuclei. For the case of the  $\bar{\nu}$ , around the peak positions, the effects of the density dependence reduce the cross sections by about 20% for  $\rho = 0.5\rho_0$ , 35% for  $\rho = 1.0\rho_0$ , 50% for  $\rho = 1.5\rho_0$ , and 60% for  $\rho = 2.0\rho_0$ . The effect for  $\bar{\nu}$  is greater than that for  $\nu$ .

The main reason why we have density effects larger than those in the electron scattering comes from the axial form factor peculiar to the  $\nu$  scattering. As shown in Fig. 1 in

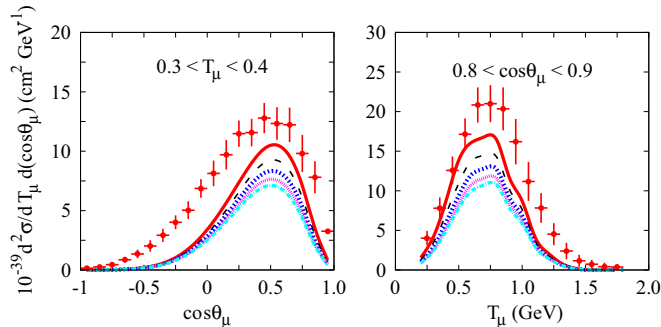


FIG. 3. (Color online) The double cross sections of the neutrino scattering in terms of the muon angle (left panel) and the muon kinetic energy (right panel). The experimental data were measured by MiniBooNE [15].

the second paper of Ref. [14], the axial form factor shows stronger momentum and density dependence than those of vector form factors, if we exploit the QMC form factor. For example, around a density of  $\rho = 1.0\rho_0$ , about 15% is changed for the axial form factor while about 10% change happens for EM form factors.

In Fig. 3, we calculate the double-differential cross sections as a function of the outgoing muon angle (left panel) and muon kinetic energy (right panel). The explanations of the curves are the same as for Fig. 2. The effects of the density dependence are the same as for the previous results in Fig. 2. For the case of no density dependence, our results are smaller than the MiniBooNE data [15] by about 20% around the peak.

In Fig. 4(a), we calculate the total cross sections of Eq. (1) for  $^{12}\text{C}(\nu_\mu, \mu^-)$  scattering in terms of the incident  $\nu$  energies and compare our results with the experimental data from MiniBooNE [15]. We use the standard axial mass  $M_A = 1.032$  GeV. The in-medium effects by the density dependent form factors reduce the total cross sections by about 10% for  $\rho = 0.5\rho_0$ , 15% for  $\rho = \rho_0$ , 20% for  $\rho = 1.5\rho_0$ , and 18% for  $\rho = 2.0\rho_0$ . The red line, which is the RMF calculation by the form factors in free space, is already too small by about 40% by comparing with the experimental data. Discussions on the final-state interaction by other approaches are detailed in other papers. If we consider the nuclear density of  $^{12}\text{C}$  as about

$0.6\rho_0$ , the discrepancy becomes about 60% by comparing with the data.

To reduce this discrepancy, we use the different value of the axial mass  $M_A = 1.39$  GeV fit to another MiniBooNE experiment [25] in Fig. 4(b). The experiment is for the  $\nu$  elastic scattering from  $\text{CH}_2$  via NC. The effect of the different axial mass  $M_A$  enhances the total cross sections about 32%; that is, the effect of  $M_A$  is about 35%. The effect of the density dependence is the same as in the previous figure. But our results are still below the experimental data. However, the discrepancy becomes larger by about 15% if the density dependencies of the form factors are taken into account as  $\rho = \rho_0$ .

In this work, we investigate the density dependence on the differential cross sections for the  $(e, e')$  reaction and the CC reaction of  $A(\nu_\mu, \mu^-)$  and  $A(\bar{\nu}_\mu, \mu^+)$  scattering within the framework of a relativistic single-particle model. The effect of the density dependence enhances the  $(e, e')$  cross section by about a few percent and reduces the  $\nu$ - $A$  cross sections around peak positions by about 10% for  $\rho = 0.5\rho_0$  but the effect for the  $\bar{\nu}$ - $A$  scattering reduces up to 20%. The in-medium effects are 20% to 30% even for the case of  $\bar{\nu}$  if one considers the density of finite nuclei,  $^{12}\text{C}$ ,  $^{40}\text{Ca}$ , and  $^{208}\text{Pb}$  as  $0.6\rho_0$ ,  $0.7\rho_0$ , or  $1.0\rho_0$ , respectively. Our theoretical double-differential cross sections with free-space values are smaller than the experimental data by about 20%. The effects of the density dependence reduces the double-differential cross sections. The effect on the total cross sections is estimated to reduce them by about 15%, irrespective of axial mass  $M_A$ . Since our results for  $M_A = 1.39$  GeV are still below the experimental data by 15%, even if the in-medium effect is taken into account, we need to improve our nuclear model such as the nuclear model of the bound and the final states.

In nuclear matter, the chiral symmetry is believed to be partially restored, which implies that the quark mass is reduced depending on the density. In the QMC model used in this work, the quark mass is also reduced by the in-medium attractive scalar force due to the surrounding nucleons because it is constructed with the chiral symmetry. This is the reason why  $g_A$  is decreased in nuclear matter or in a nucleon embedded in a nucleus, as shown in Fig. 1 of our previous papers [14]. This reduction is the main reason leading to the reduction of relevant cross sections. In fact, this approach is usually

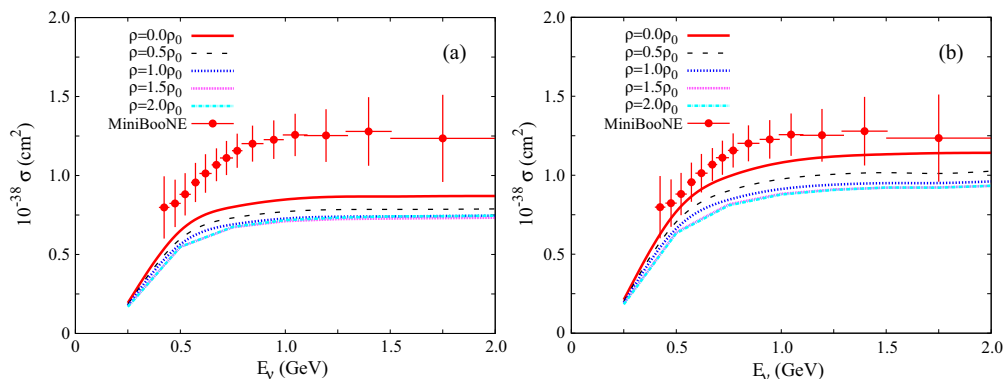


FIG. 4. (Color online) The total cross sections of the neutrino scattering in terms of the incident energies with (a)  $M_A = 1.032$  GeV and (b)  $M_A = 1.39$  GeV. The experimental data are measured by MiniBooNE [15].

adopted for infinite nuclear matter, such as neutron stars. Of course, nobody can be sure of the validity of this approach for nuclear matter because all related coupling constants are determined to reproduce static properties of finite nuclei at  $\rho = \rho_0$ . One of the motivations of this work is to test this approach for neutrino scattering in the quasi-elastic region,

although disagreement with MiniBooNE data becomes more serious.

This work was supported by the National Research Foundation of Korea (Grants No. 2012R1A1A2041974, No. 2011-0015467, and No. 2012M7A1A2055605).

- 
- [1] J. Aubert *et al.*, *Phys. Lett. B* **123**, 275 (1983); J. Ashman *et al.*, *ibid.* **206**, 364 (1988).
- [2] D. H. Lu *et al.*, *Nucl. Phys. A* **634**, 443 (1998); K. Saito, K. Tsushima, and A. W. Thomas, *Phys. Lett. B* **465**, 27 (1999).
- [3] Il-Tong Cheon and Moon Taeg Jeong, *J. Phys. Soc. Jpn.* **61**, 2726 (1992); M. T. Jeong and Il- T. Cheon, *Phys. Rev. D* **43**, 3725 (1991).
- [4] M. K. Jones *et al.*, *Phys. Rev. Lett.* **84**, 1398 (2000).
- [5] S. Dieterich *et al.*, *Phys. Lett. B* **500**, 47 (2001).
- [6] Jefferson Lab E93-049 Collaboration, S. Strauch *et al.*, *Phys. Rev. Lett.* **91**, 052301 (2003).
- [7] S. P. Malace, M. Paolone, S. Strauch, I. Albayrak, J. Arrington, B. L. Berman, E. J. Brash, and B. Briscoe *et al.*, *Phys. Rev. Lett.* **106**, 052501 (2011).
- [8] K. S. Kim and Myung-Ki Cheoun, *Phys. Rev. C* **67**, 034603 (2003).
- [9] K. S. Kim and L. E. Wright, *Phys. Rev. C* **68**, 027601 (2003).
- [10] I. C. Cloet, G. A. Miller, E. Piasetzky, and G. Ron, *Phys. Rev. Lett.* **103**, 082301 (2009).
- [11] D. H. Lu, K. Tsushima, A. W. Thomas, A. G. Williams, and K. Saito, *Phys. Lett. B* **441**, 27 (1998); D. H. Lu, A. W. Thomas, K. Tsushima, A. G. Williams, and K. Saito, *ibid.* **417**, 217 (1998); D. H. Lu, K. Tsushima, A. W. Thomas, A. G. Williams, and K. Saito, *Phys. Rev. C* **60**, 068201 (1999); D. H. Lu, A. W. Thomas, and K. Tsushima, [arXiv:nucl-th/0112001](https://arxiv.org/abs/nucl-th/0112001); A. W. Thomas, *Nucl. Phys. B, Proc. Suppl.* **112**, 57 (2002).
- [12] K. Saito, K. Tsushima, and A. W. Thomas, *Nucl. Phys. A* **609**, 339 (1996); *Phys. Rev. C* **55**, 2637 (1997).
- [13] K. Tsushima, K. Saito, J. Haidenbauer, and A. W. Thomas, *Nucl. Phys. A* **630**, 691 (1998); Pierre A. M. Guichon, Anthony W. Thomas, and Kazuo Tsushima, *ibid.* **814**, 66 (2008).
- [14] Myung-Ki Cheoun *et al.*, *Phys. Lett. B* **723**, 464 (2013); *Phys. Rev. C* **87**, 065502 (2013).
- [15] A. A. Aguilar-Arevalo *et al.* (MiniBooNE Collaboration), *Phys. Rev. D* **81**, 092005 (2010).
- [16] J. Nieves, I. Ruiz Simo, and M. J. Vicente Vacas, *Phys. Lett. B* **707**, 72 (2012).
- [17] A. Meucci, M. B. Barbaro, J. A. Caballero, C. Giusti, and J. M. Udias, *Phys. Rev. Lett.* **107**, 172501 (2011); A. Meucci, C. Giusti, and F. D. Pacati, *Phys. Rev. D* **84**, 113003 (2011).
- [18] Artur M. Ankowski, *Phys. Rev. C* **86**, 024616 (2012).
- [19] C. J. Horowitz and B. D. Serot, *Nucl. Phys. A* **368**, 503 (1981).
- [20] C. Maieron, M. C. Martinez, J. A. Caballero, and J. M. Udias, *Phys. Rev. C* **68**, 048501 (2003); M. C. Martinez, P. Lava, N. Jachowicz, J. Ryckebusch, K. Vantournhout, and J. M. Udias, *ibid.* **73**, 024607 (2006); Andrea Meucci, J. A. Caballero, C. Giusti, and J. M. Udias, *ibid.* **83**, 064614 (2011); R. Gonzalez-Jimenez, M. V. Ivanov, M. B. Barbaro, J. A. Caballero, and J. M. Udias, *Phys. Lett. B* **718**, 1471 (2013).
- [21] K. S. Kim, L. E. Wright, Yanhe Jin, and D. W. Kosik, *Phys. Rev. C* **54**, 2515 (1996); K. S. Kim, L. E. Wright, and D. A. Resler, *ibid.* **64**, 044607 (2001); K. S. Kim and L. E. Wright, *ibid.* **72**, 064607 (2005); K. S. Kim, B. G. Yu, and M. K. Cheoun, *ibid.* **74**, 067601 (2006).
- [22] K. S. Kim and Myung-Ki Cheoun, *Phys. Rev. C* **83**, 034607 (2011).
- [23] K. S. Kim, Myung-Ki Cheoun, and Byung Geel Yu, *Phys. Rev. C* **77**, 054604 (2008); K. S. Kim, B. G. Yu, M. K. Cheoun, T. K. Choi, and M. T. Chung, *J. Phys. G* **34**, 2643 (2007).
- [24] D. B. Day *et al.*, *Phys. Rev. Lett.* **59**, 427 (1987).
- [25] A. A. Aguilar-Arevalo *et al.* (MiniBooNE Collaboration), *Phys. Rev. D* **82**, 092005 (2010).